Beyond the random-phase approximation: A new approximation scheme for the polarization propagator

Jochen Schirmer

Lehrstuhl für Theoretische Chemie, Institut für Physikalische Chemie, Universität Heidelberg,
D-6900 Heidelberg, Germany
(Received 25 November 1981)

Within the framework of the many-body Green's-function method we present a new approach to the polarization propagator for finite Fermi systems. This approach makes explicit use of the diagrammatic perturbation expansion for the polarization propagator, and reformulates the exact summation in terms of a simple algebraic scheme, referred to as the algebraic diagrammatic construction (ADC). The ADC defines in a natural way a set of approximation schemes (nth-order ADC schemes) which represent infinite partial summations exact up to nth order of perturbation theory. In contrast to the random-phase-approximation (RPA)-like schemes, the corresponding mathematical procedures are essentially Hermitian eigenvalue problems in limited configuration spaces of unperturbed excited configurations. Explicit equations for the first- and second-order ADC schemes are derived. These schemes are thoroughly discussed and compared with the Tamm-Dancoff approximation and RPA schemes.

I. INTRODUCTION

The various many-body methods[1] for the excitations of finite nucleonic and electronic systems may be classified according to a few basic concepts. Perhaps the most prominent concept is the method of the many-body Green's functions.[2,3] Here, the interesting entities are the two-particle Green's function, the related particle-hole (p-h) response function[4] and the polarization propagator,[5,6] also known as p-h propagator. The Fourier transforms of these functions have poles at the excitation energies of the system under consideration, while the transition moments are related to the corresponding residues. The advantage of the Green's functions is that there exist well-defined perturbation expansions in terms of Feynman diagrams which are very useful for the construction of approximation schemes. There also exist exact equations, which allow for various approximative solutions, e.g., the hierarchy of equations of motions[7] introducing a coupling to higher Green's functions, and the Bethe-Salpeter integral equation[4,8] for the p-h-response function introducing the diagrammatically defined effective p-h-interaction.

As an alternative concept, we mention the equation of motion method (EOM).[9,10] Its basic equa-

tions are formulated in terms of ground-state expectation values of exact excitation operators. Here, approximation schemes result in a straightforward but increasingly complicated way by expanding the excitation operators and the ground state in terms of basic operators and unperturbed configurations, respectively. It is interesting to note that equivalent equations result from the so-called superoperator representation of the polarization propagator considered by several authors.[11,12]

Certainly, the fundamental approximation scheme, deriving from the many-body concepts mentioned above, as from several other approaches, is the random-phase approximation (RPA)[13,14] which has long been applied to nuclei,[15] atoms,[16] and molecules.[17] The RPA can be viewed as an infinite though only partial summation of terms in the perturbation expansion of the polarization propagator. It is recognized[9] that the RPA excitation energies and transition moments are exact up to first order of perturbation theory (with respect to the two-particle interaction). However, the corrections introduced by the RPA in second and higher order are selective and, so far as the excitation energies are concerned, may lead to poorer results than obtained in the simpler Tamm-Dancoff approximation (TDA). Mathematically, the RPA represents a non-Hermitian (pseudo) eigenvalue

problem,[14] where the configuration space consists of the single or particle-hole (p-h) excitations with respect to the unperturbed (Hartree-Fock) ground state plus the "unphysical" hole-particle (h-p) excitations. As a consequence of the non-hermiticity there may occur complex solutions[14] for the energies of low-lying excited states (Hartree-Fock "instabilities") which, of course, is a rather undesirable feature.

The RPA has successfully been applied in nuclear physics (for an overview see Ring and Schuck[18]). Since here a precise nucleon-nucleon interaction potential is not available, one usually employs model potentials with adjustable parameters. For atoms and molecules, on the other hand, the electron-electron interaction is given by the familiar Coulomb potential being well amenable to a numerical treatment. Here the comparison of the RPA calculations with experimental results allows a direct conclusion about the accuracy of the method. As the early applications[16,17] have already demonstrated, the RPA gives rather disappointing results for the excitation energies. Typical deviations from the experimental results for small molecules (N_2) are in the order of magnitude of 1 eV (see, e.g., Rose et al.[19]). Clearly, this accuracy cannot match the outcome of an even moderate configuration interaction (CI) treatment. For the transition moments the situation is more satisfactory: the RPA achieves a significant improvement with respect to Hartree-Fock (HF) and TDA results. Actually, most RPA applications in atomic and molecular physics are concerned with transition properties (for a recent review and references we refer to the article of Oddershede[12]).

Various attempts have been made to develop extended approximations.[9,20-28] Most of these schemes have in common that they follow the lines prescribed by the RPA, that is, they maintain the pseudo-eigenvalue problem in a space comprising both physical and unphysical configurations. For example, in the EOM approach, one may extend the expansion of the basic operators to include the physical 2p-2h excitations plus the unphysical 2h-2p excitations.[23,28] In order to be consistent through a finite order of perturbation theory one is forced to take further unphysical excitations, e.g., p-p and h-h excitations into account, and to use a larger expansion of the ground state.[23,27,28] This introduces nonorthogonality for the basic excitations necessitating rather complicated formulas. The explicit consideration of the unphysical excitations leads soon to undersirably large configuration spaces and actual calculations become very expensive. On the other hand, the results of the extended RPA-like approximations (a useful compilation for atoms and molecules is given by Oddershede[12]) are, in general, not as rewarding as one might expect from the effort involved.

It is the purpose of this article to present a new approach the spirit of which is completely different from that of the RPA as are the resulting mathematical procedures. For reasons which will become clear below, this approach will be called the algebraic diagrammatic construction (ADC). Here, one starts explicitly from the diagrammatic perturbation expansion of the polarization propagator (more precisely, of the so-called transition function being equivalent to the polarization propagator for a general transition operator). We present a simple algebraic scheme by which (in principle) this expansion can be summed. This scheme allows immediate definition of approximations which represent infinite partial summations being exact up to a finite, say nth, order of perturbation theory. We shall present the explicit construction of these "nth order ADC schemes" for $n = 0$, 1, and 2. The important feature is that the resulting mathematical procedures involve only Hermitian eigenvalue problems within limited spaces of physical excitations, i.e., p-h, 2p-2h, . . ., excitations. For example, the first-order ADC scheme is formulated in the space of the p-h excitations. Since this approximation yields the excitation energies and the transition moments (for singly excited states) consistent through first-order it can be viewed as an analog to the RPA. The second-order ADC employing both the p-h and 2p-2h excitations is clearly beyond the capabilities of the RPA. It gives results which are exact up to second order for the singly excited states. It also yields higher (2p-2h) excited states which can be treated consistently through first order. These properties give rise to the expectation that the second-order ADC scheme will represent a very useful approximation for actual applications.

The plan of this article is as follows. In Sec. II we shall give a short review of the theory of the polarization propagator and provide for the essential definitions. The general ADC scheme and the explicit construction of the zeroth-, first-, and second-order approximations are presented in Sec. III. Section IV is devoted to a discussion of these schemes. Here the ADC results are analyzed by comparing them with the TDA, the RPA, and the first orders of Rayleigh-Schrödinger perturbation theory. A short summary is given in the final Sec. V.

II. THE PARTICLE-HOLE (p-h) PROPAGATOR

A. Definitions

Within the many-body Green's function approach the central entity for the excitation problem is the particle-hole (p-h) response function[4]

$$R_{12,1'2'} = G_{12,1'2'} - G_{11'}G_{22'} ,$$ (1)

where the one- and two-particle Green's functions are defined according to[2]

$$G_{11'} = -i\langle \Psi_0 | \hat{T} c_1(t_1) c_{1'}^\dagger(t_{1'}) | \Psi_0 \rangle ,$$ (2a)

$$G_{12,1'2'} = (-i)^2 \langle \Psi_0 | \hat{T} c_1(t_1) c_2(t_2) c_{2'}^\dagger(t_{2'}) c_{1'}^\dagger(t_{1'}) | \Psi_0 \rangle .$$ (2b)

Here, $|\Psi_0\rangle$ denotes the exact ground state of the considered fermion system, $c_i^\dagger(t)$ $[c_i(t)]$ are one-particle creation (destruction) operators in the Heisenberg representation associated with suitably chosen one-particle states $|i\rangle$, e.g., Hartree-Fock states. Throughout this article we shall make no formal distinction between discrete and continuum one-particle states. $\hat{T}$ denotes the time-ordering operator introducing step functions of time arguments, on the right-hand side of Eqs. (2),

$$\Theta(\tau) = \begin{cases} 0 , & \tau < 0 \\ e^{-\eta\tau} , & \tau \geq 0 \end{cases}$$

which include a positive infinitesimal η in order to guarantee the convergence of the Fourier transforms.[29]

The p-h-response function R is subject to the Bethe-Salpeter equation[4,8]

$$R_{12,1'2'} = -G_{12'}G_{21'} - iG_{13}G_{41'}K_{43',34'}^{p\text{-}h}R_{3'2,4'2'} .$$ (3)

In this shorthand notation, summation and time integration for doubly occurring indices is implied. The effective p-h interaction $K^{p\text{-}h}$ can be defined diagrammatically as the irreducible p-h vertex[2,4] or by functional derivatives of simpler entities.[7] Since the exact $K^{p\text{-}h}$ depends on four time arguments (or three time differencies), Eq. (3) represents, both in time and in ω space, a very complicated integral equation. Many attempts to solve Eq. (3) by introducing approximations for $K^{p\text{-}h}$ as well as for the one-particle Green's function G have been reported in the literature.[4,30] Certainly, the most fundamental approach is the RPA,[14] which is obtained by employing the first-order approximation (with respect to the two-particle interaction) for $K^{p\text{-}h}$ and by replacing the one-particle Green's functions G by the "free" (zeroth-order perturbation theory) Green's functions G^0. We shall discuss this approximation in more detail in Sec. IV.

Whereas for the Bethe-Salpeter equation (3) the full p-h response function with its dependence on three time arguments is needed, its physical information is already contained in the simpler p-h propagator[5,6] (or polarization propagator) defined by

$$\Pi_{jk,j'k'}(t,t') = \lim_{\substack{t_j,t_k \to t \\ t_{j'},t_{k'} \to t'}} iR_{jk',kj'}(t_j,t_{k'},t_k,t_{j'}) .$$ (4)

As one may ascertain from the definitions (1) and (2) the result of the right-hand side does not depend on the time ordering of the limits. For a time-independent Hamiltonian the p-h-propagator is a function of the time difference $t - t'$ only. Its Fourier transform

$$\Pi_{jk,j'k'}(\omega) = \int_{-\infty}^{\infty} d(t-t') e^{i\omega(t-t')} \Pi_{jk,j'k'}(t,t')$$ (5)

has the spectral representation

$$\Pi_{jk,j'k'}(\omega) = \sum_{m\neq 0} \frac{\langle \Psi_0 | c_k^\dagger c_j | \Psi_m \rangle \langle \Psi_m | c_{j'}^\dagger c_{k'} | \Psi_0 \rangle}{\omega + E_0 - E_m + i\eta} + \sum_{m\neq 0} \frac{\langle \Psi_0 | c_{j'}^\dagger c_{k'} | \Psi_m \rangle \langle \Psi_m | c_k^\dagger c_j | \Psi_0 \rangle}{-\omega + E_0 - E_m + i\eta} .$$ (6)

Here E_m and $|\Psi_m\rangle$ denote, respectively, the energies and the wave functions of the excited states. It should be noted that the summation on the right-hand side of Eq. (6) does not include the ground state $|\Psi_0\rangle$. This is due to the subtraction of the product $G_{11'}G_{22'}$ in the definition of R according to (1). From the spectral representation (6) it is clear that, $\underline{\Pi}(\omega)$ (employing a compact matrix notation) is the sum of two parts

$$\underline{\Pi}(\omega) = \underline{\Pi}_+(\omega) + \underline{\Pi}_-(\omega) , \tag{7}$$

which are analytic in the upper and lower halves of the complex plane, respectively. These parts are interrelated by

$$\underline{\Pi}_+^\dagger(-\omega) = \underline{\Pi}_-(\omega) , \tag{8}$$

i.e., $\underline{\Pi}_-(\omega)$ and thus $\underline{\Pi}(\omega)$ are given once $\underline{\Pi}_+(\omega)$ is known. In particular, the entire physical information is already included in each of the two parts. It should be noted that, by the contour integration

$$\underline{\Pi}_+(\omega) = \frac{1}{2\pi i} \int \frac{d\omega'}{\omega' - \omega - i\eta} \underline{\Pi}(\omega') . \tag{9}$$

$\underline{\Pi}_+(\omega)$ can be projected out of the full propagator $\underline{\Pi}$. The contour, here, closes in the upper complex plane.

We finally discuss the physical information contained in the polarization propagator $\underline{\Pi}(\omega)$. According to the spectral representation (6) the excitation energies $\Delta E_m = E_m - E_0$ are given by the poles of $\underline{\Pi}_+(\omega)$. The corresponding transition moments

$$T_m = \langle \Psi_m | \hat{D} | \Psi_0 \rangle \tag{10}$$

for a general one-particle transition operator $\hat{D}$ reading in second-quantized notation

$$\hat{D} = \sum D_{rs} c_r^\dagger c_s \tag{11}$$

are obtained from the matrix of residues

$$\underline{P}_m = \lim_{\omega \to E_m - E_0} (\omega + E_0 - E_m) \underline{\Pi}_+(\omega) ; \tag{12}$$

according to

$$|T_m|^2 = \underline{D}^\dagger \underline{P}_m \underline{D} . \tag{13}$$

Here, $\underline{D}$ denotes the column vector of matrix elements D_{rs}. In a notation which also applies for transitions to continuum states the spectral function,

$$f(\omega) = \sum_m |T_m|^2 \delta(\omega + E_0 - E_m) \tag{14}$$

may be written as

$$f(\omega) = -\frac{1}{\pi} \text{Im} T(\omega) , \tag{15}$$

where

$$T(\omega) = \underline{D}^\dagger \underline{\Pi}_+(\omega) \underline{D} \tag{16}$$

is referred to as the transition function of the operator $\hat{D}$.

B. Diagrammatic perturbation theory for the polarization propagator

As is widely known, there exist well-established perturbation expansions for the n-particle Green's functions which may be formulated in terms of Feynman diagrams.[2,6] These perturbation expansions make use of the usual partitioning of the full Hamiltonian

$$\hat{H} = \hat{H}_0 + \hat{H}_I = \hat{H}_0 + \hat{W} + \hat{V} ,$$
$$\hat{H}_0 = \sum \epsilon_i c_i^\dagger c_i , \tag{17}$$
$$\hat{H}_I = \sum W_{ij} c_i^\dagger c_j + \frac{1}{2} \sum V_{ijkl} c_i^\dagger c_j^\dagger c_l c_k ,$$

into a diagonal one-particle part $\hat{H}_0$ and an interaction part $\hat{H}_I$ consisting of a nondiagonal one-particle part $\hat{W}$ and the two-particle interaction part $\hat{V}$. Here

$$V_{ijkl} = \langle \phi_i(1)\phi_j(2) | V(1,2) | \phi_k(1)\phi_l(2) \rangle \tag{18}$$

denote the matrix elements of the two-particle interaction (e.g., Coulomb interaction) with respect to the one-particle states $|\phi_i\rangle$. For simplicity we shall assume a formulation in terms of Hartree-Fock (HF) one-particle states. In this case the ϵ_i are the HF orbital energies and the matrix elements W_{ij} are given by

$$W_{ij} = -\sum_k V_{ik[jk]} n_k . \tag{19}$$

Here n_k denote HF occupation numbers, i.e., $n_k = 1(0)$ for $|\phi_k\rangle$ occupied (unoccupied) in the HF ground state. It is also useful to define $\bar{n}_k = 1 - n_k$. The antisymmetrized matrix element $V_{ij[kl]} = V_{ijkl} - V_{ijlk}$ is used in Eq. (19). We stress that the choice of the HF one-particle Hamiltonian $H_0 = H_{HF}$ does not restrict the generality of the following considerations. The formulation for non-HF one-particle states is, though more lengthy, a straightforward extension of the HF case.

The diagrammatic perturbation expansion for the p-h propagator $\underline{\Pi}(t,t')$ may be derived according to the general procedure (see, e.g., Fetter and Walecka[6]) from the expression

$$\Pi_{jk,j'k'}(t,t') = -i\langle\Psi_0|\hat{T}c_k^\dagger(t)c_j(t)c_{j'}^\dagger(t')c_{k'}(t')|\Psi_0\rangle + i\langle\Psi_0|c_k^\dagger(t)c_j(t)|\Psi_0\rangle\langle\Psi_0|c_{j'}^\dagger(t')c_{k'}(t')|\Psi_0\rangle , \qquad (20)$$

which follows from Eqs. (1), (2), and (4). The second part on the right-hand side, simply cancels a certain class of diagrams stemming from the first part, namely, all "disjoint" diagrams[6] which are characterized by the structure shown in Fig. 1. The diagrammatic expansion for $\underline{\Pi}(t,t')$ up to second order (using the Abrikosov notation) is shown in Fig. 2. The precise rules for drawing and evaluating the diagrams are given in Appendix A. A pictorial explanation of the graphical symbols is given in Fig. 3. The solid lines represent (zeroth-order) free one-particle Green's functions

$$G_{kk'}^0(t,t') = -\delta_{kk'}ie^{-i\epsilon_k(t-t')}[\bar{n}_k\Theta(t-t') - n_k\Theta(t'-t)] . \qquad (21)$$

This expression follows from the definition Eq. (2a), when the free (HF) Hamiltonian $\hat{H}_0$ and the corresponding unperturbed (HF) ground state $|\phi_0\rangle$ are employed.

The evaluation of a nth order Feynman diagram $A(t,t')$ requires n time integrations over the internal time arguments $t_1, \ldots, t_n$. The result of these integrations and of the Fourier transformation

$$A(\omega) = \int_{-\infty}^{\infty}e^{i\omega(t-t')}A(t,t')d(t-t') \qquad (22)$$

can be read directly off the $(n+2)!$ so-called Goldstone diagrams which result from the graph of A by drawing all different orderings of the $n+2$ vertices $t,t_1, \ldots, t_n,t'$. Again, the rules for evaluating the Goldstone diagrams are listed in Appendix A. The $(n+2)!$ time-ordered Goldstone diagrams for a given Feynman diagram can be divided into two separate classes of diagrams according to the ordering of the external times $t > t'$ and $t < t'$, respectively. It is easily established that the first class $(t > t')$ contributes exclusively to the part $\underline{\Pi}_+(\omega)$ of the p-h propagator and the second class $(t < t')$ contributes exclusively to $\underline{\Pi}_-(\omega)$. There are no mixed terms and one can calculate $\underline{\Pi}_+(\omega)$ and $\Pi_-(\omega)$ independently, as might be expected from the fact that both parts contain identical physical information. In Figs. 5 and 6 the first- and second-order Goldstone diagrams contributing to $\underline{\Pi}_+(\omega)$ are displayed.
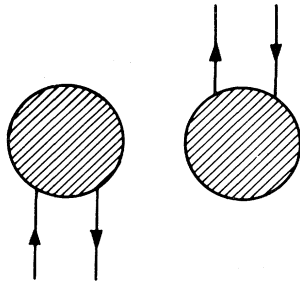
FIG. 1. Disjoint diagrams contributing to the first term of the right-hand side of Eq. (20).

III. THE ALGEBRAIC DIAGRAMMATIC CONSTRUCTION

In the following we present a new approximation scheme for the polarization propagator, which will be referred to as the algebraic diagrammatic construction (ADC). We will start by discussing the general idea of the ADC in Sec. III A. In Sec. III B we present the explicit construction of the first- and second-order ADC schemes, that is, schemes which are exact up to first and second order of perturbation theory, respectively.

A. The basic concept of the ADC

The basic function considered in the following is the transition function

$$T(\omega) = \underline{D}^\dagger\underline{\Pi}_+(\omega)\underline{D} \qquad (23)$$

introduced by Eq. (16). As we have seen, this function contains the complete spectral information for the excitation process associated with the transition operator $\hat{D}$. Furthermore, there is a formal equivalence between the transition function $T(\omega)$ and the polarization propagator $\underline{\Pi}(\omega)$, if the transition operator $\hat{D}$ is taken to be completely general. Clearly, the matrix elements D_{rs} of $\hat{D}$ may be considered as variables and $T(\omega)$ represents a quadratic form of these variables. A specific matrix element of the polarization propagator, for example, $\Pi_{pq,p'q'}$, is immediately obtained by setting $D_{pq} = D_{p'q'} = 1$ and $D_{rs} = 0$, else in $T(\omega)$.

As has been discussed above, the index space of the vector $\underline{D}$ and the matrix $\underline{\Pi}_+$ comprises all pairs (r,s) of one-particle quantum numbers. According to the distinction between occupied (hole) and unoccupied (particle) one-particle states the index space may be partitioned into p-h, h-p, p-p, and h-h subspaces. This partitioning of $T(\omega)$ according to Eq. (23) is visualized in Fig. 4(a).

Via Eq. (23) the perturbation expansion for
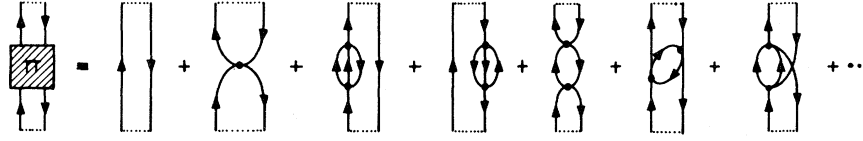
FIG. 2. Graphical representation of the polarization propagator as a sum of Feynman diagrams (in Abrikosov notation). All diagrams up to second order are shown.

$\underline{\Pi}_+(\omega)$ immediately induces a perturbation expansion for $T(\omega)$

$$T(\omega) = \sum_{n=0}^{\infty} T^{(n)}(\omega) , \tag{24a}$$

$$T^{(n)}(\omega) = \underline{D}^{\dagger} \underline{\Pi}_+^{(n)}(\omega) \underline{D} . \tag{24b}$$

As has been discussed in Sec. II, the terms of the perturbation expansion for $\underline{\Pi}_+(\omega)$ are most conveniently formulated within the diagrammatic approach. The diagrammatic rules can readily be extended to the terms $T^{(n)}(\omega)$ (see Appendix A).

Now, the basic assertions of the ADC are stated as follows:

(1) The exact transition function $T(\omega)$ can be written in the form

$$T(\omega) = \underline{F}^{\dagger} \underline{\Gamma}(\omega) \underline{F} . \tag{25a}$$

Here, the matrix $\underline{\Gamma}(\omega)$ is given by

$$\underline{\Gamma}(\omega) = [\omega \underline{1} - \underline{K} - \underline{C}]^{-1} , \tag{25b}$$

where $\underline{K}$ and $\underline{C}$ are constant (ω-independent) Hermitian matrices specified below and $\underline{F}$ denotes a vector of "modified" transition moments, i.e., linear forms of the original transition matrix elements. We note, that, strictly speaking, the infinitesimal $+i\eta$ should be added to the variable ω on the right-hand side of Eq. (25b). However, for notational brevity the $+i\eta$ is dropped, whenever unessential.

(2) The vector $\underline{F}$ and the matrices $\underline{\Gamma}$, $\underline{K}$, and $\underline{C}$ are defined within the familiar space of singly, doubly, triply, . . ., excited configurations with respect to the uperturbed (HF) ground state.
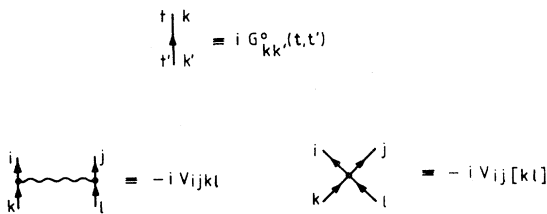
FIG. 3. Definition of the graphical symbols in the diagrams.

Within the terminology of the second quantization we shall also refer to these configurations as p-h (particle-hole), $2p$-$2h$, $3p$-$3h$, . . . , excitations. The matrix $\underline{K}$ denotes the diagonal matrix of the zeroth-order excitation energies, e.g.,

$$K_{jk,jk} = \epsilon_j - \epsilon_k , \quad \bar{n}_j n_k = 1 \tag{26}$$

$$K_{ijkl,ijkl} = \epsilon_i + \epsilon_j - \epsilon_k - \epsilon_l, \quad \bar{n}_i \bar{n}_j n_k n_l = 1 , \tag{27}$$

etc.

(3) The elements of $\underline{F}$ and of $\underline{C}$ (the matrix of the "modified" interaction) are defined by perturbation expansions in the two-particle interaction matrix elements. We denote the total contributions up to nth order by

$$\underline{F}(n) = \sum_{\gamma=0}^{n} \underline{F}^{(\gamma)} , \tag{28a}$$

$$\underline{C}(n) = \sum_{\gamma=1}^{n} \underline{C}^{(\gamma)} . \tag{28b}$$
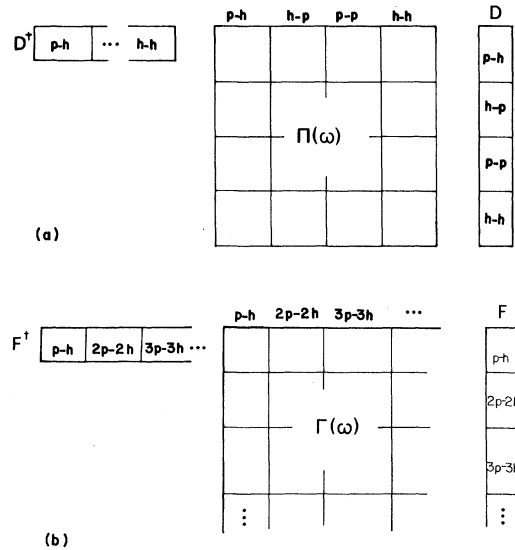
FIG. 4. (a) Graphical representation of the transition function $T(\omega)$ according to Eq. (23). (b) The transition function $T(\omega)$ according to the ADC scheme of Eq. (25).

We note, that $\underline{C}$ starts with the first-order term. The matrix $\underline{K}$ can be considered as the zeroth-order term.

(4) The perturbation expansions for $\underline{F}$ and $\underline{C}$ can successively be determined by requiring that the "nth order transition functions"

$$T_n(\omega) = \underline{F}^\dagger(n)[\omega\underline{1} - \underline{K} - \underline{C}(n)]^{-1}\underline{F}(n) , \qquad (29)$$

which are obtained when $\underline{F}(n)$ and $\underline{C}(n)$ are used in Eq. (25), are exact up to nth order, that is,

$$T_n(\omega) = \sum_{\nu=0}^{n} T^{(\gamma)}(\omega) + O(V^{n+1}) . \qquad (30)$$

It should be mentioned that this requirement is still not sufficient to construct unique expressions for $\underline{F}(n)$ and $\underline{C}(n)$. However, there is a distinguished choice, suggested by the diagrammatical perturbation expansion, as will be discussed below.

It is clear that each pair $\underline{F}(n)$ and $\underline{C}(n)$, $n = 0,1,2,\ldots$, constructed in this way defines an approximation for the transition function $T(\omega)$ and for the polarization propagator $\underline{\Pi}(\omega)$. These approximations referred to as the nth order ADC schemes represent infinite partial summations for the diagrammatic perturbation expansions being exact up to nth order perturbation theory. For a given $\underline{F}(n)$ and $\underline{C}(n)$ the matrix inversion in Eq. (25b) is equivalent to the (Hermitian) eigenvalue problem

$$(\underline{K} + \underline{C})\underline{X} = \underline{X}\underline{\Omega} , \qquad (31)$$

where $\underline{\Omega}$ and $\underline{X}$ denote the diagonal matrix of eigenvalues and the eigenvector matrix, respectively. The corresponding transition functions [according to Eq. (25a)], reads

$$T(\omega) = \underline{F}^\dagger\underline{X}(\omega\underline{1} - \underline{\Omega})^{-1}\underline{X}^\dagger\underline{F} . \qquad (32)$$

The required configuration space for the nth order ADC scheme is restricted to the lowest excited configurations. As will be seen in Sec. III B, the (trivial) zeroth-order ADC is formulated within the space of p-h excitations (singly excited configurations). This is also the case for the first-order ADC. For the second-order scheme, in addition to the p-h excitations, one has to include the space of $2p$-$2h$ excitations. The highest excited configurations which have explicitly to be taken into account for the nth order ADC are mp-mh excitations, where $m = \frac{1}{2}n + 1$ for n even and $m = \frac{1}{2}(n-1) + 1$ for n odd. Figure 4(b) is a graphical representation of the ADC scheme for the transition function.

So far assertions (1)–(4) of the ADC scheme

have not been justified and we shall shortly discuss the questions of a general proof. It may appear quite astonishing that all terms of the complicated diagrammtic perturbation expansion for $T(\omega)$ can be collected within the simple matrix scheme of Eq. (25). Actually, however, the first three assertions are almost trivial. To see this one may consider the expression for the exact transition function

$$T(\omega) = \underline{T}^\dagger[\omega\underline{1} - \underline{\Delta}]^{-1}\underline{T} , \qquad (33)$$

which is obtained from the spectral representation (6) of the polarization propagator. Here $\underline{\Delta}$ denotes the diagonal matrix of the exact excitation energies

$$\Delta E_m = E_m - E_0 , \qquad (34)$$

and $\underline{T}$ is the vector of the exact transition moments

$$T_m = \langle \Psi_m | \hat{D} | \Psi_0 \rangle . \qquad (35)$$

We note that the space of the exact excited states $| \Psi_m \rangle$ is isomorphic to the space of the unperturbed excited configurations. Obviously, Eq. (33) represents a special case of the form which has been postulated for $T(\omega)$ in Eq. (25), namely, a form where the modified interaction matrix $\underline{C}^\Delta$ according to

$$\underline{\Delta} = \underline{K} + \underline{C}^\Delta \qquad (36)$$

is diagonal. It is also clear that in accordance with point (3), both the components of $\underline{T}$ and of $\underline{C}^\Delta$ have perturbation expansions, namely, the familiar Rayleigh-Schrödinger perturbation expansions for the excitation energies ΔE_m and the transition moments T_m, respectively. The general form of Eq. (25) for $T(\omega)$,

$$T(\omega) = \underline{F}^\dagger[\omega\underline{1} - \underline{K} - \underline{C}]^{-1}\underline{F} , \qquad (37)$$

with a nondiagonal matrix C, is readily obtained from Eq. (33) by replacing $\underline{T}$ and $\underline{\Delta}$ by "transformed" entities

$$\underline{F} = \underline{Y}\underline{T} \qquad (37a)$$

and

$$\underline{K} + \underline{C} = \underline{Y}\underline{\Delta}\underline{Y}^\dagger , \qquad (37b)$$

respectively, where $\underline{Y}$ is a unitary matrix

$$\underline{Y}^\dagger\underline{Y} = \underline{1} . \qquad (37c)$$

Assuming that $\underline{Y}$ can be expanded formally in a perturbation expansion, the components of $\underline{F}$ and $\underline{C}$ have perturbation expansions as well, as is stated in point (3).

From the above discussion it is apparent that the modified transition moments $\underline{F}$ and the matrix $\underline{C}$ of Eq. (25) are not uniquely determined. Indeed, any choice of the unitary matrix $\underline{Y}$ yields, via Eq. (37), compatible expressions $\underline{F}$ and $\underline{C}$. Thus, it turns out that the nontrivial part of the ADC scheme is connected with the determination of $\underline{F}$ and $\underline{C}$ up to a certain order according to point (4). Indeed, as we shall see explicitly up to second order, the comparison of the nth order transition function $T_n(\omega)$ of Eq. (29) with the perturbation expansion of $T(\omega)$ up to nth order [Eq. (30)] does not yield an unique result for $\underline{F}$ and $\underline{C}$, thus reflecting the nonuniqueness of the expressions (37) for $\underline{F}$ and $\underline{C}$. The decisive point, however, is that the diagrammatic perturbation expansion of $T(\omega)$ represents a distinguished form, which, in turn, induces a well-defined choice for $\underline{F}(n)$ and $\underline{C}(n)$. We shall demonstrate this up to $n = 2$ by the explicit constructuion of the zeroth, first- and second-order expressions for $\underline{F}$ and $\underline{C}$ in Sec. III B. A general proof of this diagrammatic construction and, in particular, closed analytical expressions for the resulting entities $\underline{F}$ and $\underline{C}$ are not yet available.

We note that another distinguished choice of $\underline{F}$ and $\underline{C}$ results if one requires $\underline{C}$ to be diagonal. In this case one arrives necessarily at Eq. (33), where $\underline{F}$ is the vector $\underline{T}$ of the exact transition moments [Eq. (35)] and $\underline{C}$ is determined by Eq. (36). Here, the comparison of the nth order transition functions with the perturbation expansion of $T(\omega)$ yields directly the Rayleigh-Schrödinger expansions for the transition moment T_m and the excitation energies ΔE_m up to nth order. This procedure may be regarded as a diagrammatic construction of the Rayleigh-Schrödinger perturbation theory for excited states.

B. Explicit construction of the ADC schemes

1. Zeroth and first order

The zeroth-order diagram for $T(\omega)$ [or $\underline{\Pi}_+(\omega)$] is given in Fig. 2. The corresponding analytical expression reads

$$T^{(0)}(\omega) = \sum_{j,k} D_{jk}^* \frac{\bar{n}_j n_k}{\omega + \epsilon_k - \epsilon_j} D_{jk} \ . \tag{38}$$

Here, j and k denote particle and hole states, respectively. Clearly, the right-hand side can be written in the form of Eq. (29)

$$T_0(\omega) = \underline{F}^\dagger(0)[\omega \underline{1} - \underline{K}]^{-1} \underline{F}(0) \ , \tag{39}$$

where

$$K_{jk,j'k'} = \delta_{jj'} \delta_{kk'} (\epsilon_j - \epsilon_k) \ , \tag{40a}$$

$$F_{jk}(0) = D_{jk} \ . \tag{40b}$$

Here, the configuration space is the space of singly excited configurations (p-h excitations), i.e., $\bar{n}_j n_k = \bar{n}_{j'} n_{k'} = 1$.

In first order we have to consider the expression

$$T_1(\omega) = \underline{F}(1)^\dagger [\omega \underline{1} - \underline{K} - \underline{C}]^{-1} \underline{F}(1) \ , \tag{41}$$

where according to definition (28)

$$\underline{F}(1) = \underline{F}^{(0)} + \underline{F}^{(1)} \ , \tag{42a}$$

$$\underline{C}(1) = \underline{C}^{(1)} \ . \tag{42b}$$

We now expand $T_1(\omega)$ up to first order:

$$T_1(\omega) = \underline{F}^{(0)\dagger}(\omega \underline{1} - \underline{K})^{-1} \underline{F}^{(0)} + \underline{F}^{(0)\dagger}(\omega \underline{1} - \underline{K})^{-1} \underline{C}^{(1)}(\omega \underline{1} - \underline{K})^{-1} \underline{F}^{(0)}$$

$$+ \underline{F}^{(1)\dagger}(\omega \underline{1} - \underline{K})^{-1} \underline{F}^{(0)} + \underline{F}^{(0)\dagger}(\omega \underline{1} - \underline{K})^{-1} \underline{F}^{(1)} + O(2) \ . \tag{43}$$

The first term on the right-hand side is the zeroth-order term which has already been identified with $T^{(0)}(\omega)$ above. The remaining three first-order terms have to be compared with the diagrammatic first-order contribution $T^{(1)}(\omega)$. According to Fig. 5 there occur three first-order diagrams $X(1) - X(3)$ for $T(\omega)$. The explicit expressions can easily be read off these diagrams.

$$X(1) \equiv \sum_{\substack{j,k \\ j',k'}} D_{jk}^* \frac{\bar{n}_j n_k}{(\omega + \epsilon_k - \epsilon_j)} (-V_{jk'[j'k]}) \frac{\bar{n}_{j'} n_{k'}}{\omega + \epsilon_{k'} - \epsilon_{j'}} D_{j'k'} \ , \tag{44a}$$

$$X(2) = X(3)^* = \sum_{j,k} \sum_{r,s} \frac{D_{rs}^* V_{js[rk]}^*}{\epsilon_j + \epsilon_s - \epsilon_k - \epsilon_r} n_s n_r \frac{\bar{n}_j n_k}{\omega + \epsilon_k - \epsilon_j} D_{jk} \ . \tag{44b}$$

X(1)   X(2)   X(3)
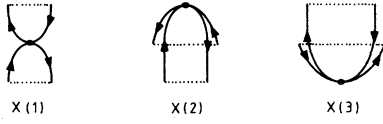
FIG. 5. First-order Goldstone diagrams (in Abriko-sov notation). The first three diagrams (out of six) con-tributing to the $+i\eta$ part $\underline{\Pi}_+$ are shown, the other dia-grams are obtained by turning round these. The dotted lines indicate the external vertices.

It is apparent that these terms fit directly into the general algebraic scheme of Eq. (43), defining $\underline{F}(1)$ and $\underline{C}(1)$:

$$C_{jk,j'k'}(1) = -V_{jk'[j'k]} , \tag{45a}$$

$$F_{jk}(1) = D_{jk} + \sum_{r,s} \frac{V_{js[rk]}\bar{n}_s n_r}{\epsilon_j + \epsilon_s - \epsilon_k - \epsilon_r} D_{rs} , \tag{45b}$$

where

$$\bar{n}_j n_k = \bar{n}_{j'} n_{k'} = 1 .$$

These expressions together with Eq. (41) constitute the first-order ADC scheme. This approximation represents an infinite partial summation for $T(\omega)$ being exact up to first order. The required config-uration space is the space of the p-h excitations. We mention here that the eigenvalue problem of the first-order ADC is identical with the TDA eigenvalue problem. Accordingly, both methods render the same excitation energies. In contrast to the TDA the ADC also yields the transition mo-ments exact up to first order, which is not the case for the TDA. In the latter respect the first-order ADC scheme has to be compared with the RPA which provides both the excitation energies and the transition moments consistent through first order. This is discussed in more detail in Sec. IV.

Here, it is appropriate to return to the nonuniqueness problem discussed in Sec. III A. First we note that, the form of the expressions (44) emerging from the diagrams gives a unique result for $\underline{F}(1)$ and $\underline{C}(1)$. However, one may deviate from this form by transforming quadratic terms, i.e., products of two ω denominators, into a sum of single ω denominators:

$$(\omega+\epsilon_k-\epsilon_j)^{-1}(\omega+\epsilon_{k'}-\epsilon_{j'})^{-1}=(\epsilon_j-\epsilon_k-\epsilon_{j'}+\epsilon_{k'})^{-1}[(\omega+\epsilon_k-\epsilon_j)^{-1}-(\omega+\epsilon_{k'}-\epsilon_{j'})^{-1}] \quad \text{for } (j,k)\neq(j',k') .$$

$$\tag{46}$$

Performing this partial fraction decomposition for all quadratic terms [except for the "genuine" qua-dratic terms where $(j,k)=(j',k')$] of the contribu-tion $X(1)$ [Eq. (44a)] the comparison with $T_1(\omega)$ of Eq. (43) yields a diagonal modified-interaction ma-trix $\underline{\tilde{C}}(1)$,

$$\tilde{C}_{jk,jk} = -V_{jk[jk]} , \tag{47a}$$

and the modified transition moment $\underline{\tilde{F}}(1)$,

$$\tilde{F}_{jk} = F_{jk} + \sum_{j',k'\neq(j,k)} \frac{-V_{jk'[j'k]}\bar{n}_{j'}n_{k'}}{\epsilon_j-\epsilon_k-\epsilon_{j'}+\epsilon_{k'}} D_{j'k'} , \tag{47b}$$

where F_{jk} is given by Eq. (45b). Clearly, the ex-pressions (47a) and (47b) can be identified as the first-order Rayleigh-Schrödinger expansions for the excitation energies and the transition moments, respectively. We note that this does not represent the only additional possibility, since, e.g., one may perform the partial fraction decomposition accord-ing to Eq. (46) not for all but for selected quadrat-ic terms. The partial fraction decomposition ac-

cording to Eq. (46) allows to "transfer" contribu-tions of the modified interaction matrix $\underline{C}$ of Eq. (45a) into the modified transition moments $\underline{F}$ of Eq. (45b). Conversely, as is easily seen, it is not possible to transfer contributions of $\underline{F}$ of Eq. (45b) into the modified interaction matrix $\underline{C}$. In this sense, we may say that the modified interaction matrix $\underline{C}$ of Eq. (45a) is "maximal," and, thereby, uniquely determined.

2. Second order

Similarly, we may now attack the second order problem. A glance at the second-order diagrams in Fig. 6 finds 5 Feynman diagrams A, B, C, D, and E, each generating 24 time-ordered Goldstone dia-grams of which 12 diagrams contribute to $T(\omega)$. Altogether this constitutes a manifold of 60 dia-grams for $T(\omega)$, which looks somewhat discour-aging. However, after some inspection, it is possi-ble to classify the various contributions within the

context of the ADC scheme quite easily. In order to do so it is helpful to remember (see the rules in Appendix A) that each cut between two interaction points represents an energy denominator being of the type

$$(\omega+\epsilon_k+\epsilon_l+\ldots-\epsilon_i-\epsilon_j-\ldots)^{-1},$$

if the cut lies between the two external vertex pairs, or, of the ω-independent-type

$$(\epsilon_k+\epsilon_l\ldots-\epsilon_i-\epsilon_j\ldots)^{-1}$$

if the cut lies above or below the two external vertex pairs. Here $k, l,\ldots$ and $i, j,\ldots$ correspond to hole and particle lines, respectively. By inspecting the cuts of each diagram one obtains a useful classification scheme which will facilitate the intended analysis. For example, the diagram $A(1)$ starts with a p-h denominator $(\omega+\epsilon_k-\epsilon_j)^{-1}$, continues with a 2p-2h denominator $(\omega+\epsilon_l-\epsilon_m-\epsilon_h-\epsilon_i)^{-1}$, and ends again with a p-h denominator $(\omega+\epsilon_{k'}-\epsilon_{j'})^{-1}$. Obviously, this diagram is associated with the coupling between p-h and 2p-2h excitations and its contributions can readily be traced within our matrix formalism.

In Table I we have listed all second-order terms of the transition function

$$T_2(\omega)=\underline{F}(2)^{\dagger}[\omega\underline{1}-\underline{K}-\underline{C}(2)]^{-1}\underline{F}(2), \qquad (48)$$

together with the assignation of the corresponding diagrams. As we have already seen from inspection of diagram $A(1)$ the configuration space now has to be enlarged by the 2p-2h excitations. Accordingly, it is possible to further partition the terms of Eq. (48) into p-h terms, 2p-2h terms, and p-h —2p-2h coupling terms. A corresponding distinction for the diagrams is introduced by Table I. Except for the 12 diagrams $A(7)-A(10)$, $B(7)-B(10)$, $C(7)-C(10)$ which will be discussed below, the classification of diagrams according to Table I is straightforward. Since $\underline{F}^{(0)}$, $\underline{F}^{(1)}$, and $\underline{C}^{(1)}$ for the p-h space have already been determined in zeroth and first order, many terms have simply to be verified. For example, the contribution (I) for the p-h space is just given by the diagram $C(4)$ as can easily be checked.

There are four new entities which are to be determined in second order, namely, $F_{jk}^{(2)}$ and $C_{jk,j'k'}^{(2)}$ for the p-h space, $F_{ijkl}^{(1)}$ for the 2p-2h space, and $C_{jk,i'j'k'l'}^{(1)}$ for the p-h —2p-2h coupling. Before presenting the final result we shall give a few comments on the individual terms. According to Table I, the coupling matrix elements $C_{jk,i'j'k'l'}^{(1)}$ are ob-

TABLE I. The correspondence between the second-order terms of the transition function $T_2(\omega)$ and the terms of the diagrammatic perturbation expansion according to Fig. 6.

	Second-order terms of $T_2(\omega)$	Corresponding diagrams ph space	Corresponding diagrams ph/2p2h space
(I)	$\underline{F}^{(1)\dagger}(\omega\underline{1}-\underline{K})^{-1}\underline{F}^{(1)}$	$C(4)$	$A(4),B(4),D(4),D(10),E(4),E(10)$
(II)/(II)*	$\underline{F}^{(1)\dagger}(\omega\underline{1}-\underline{K})^{-1}\underline{C}^{(1)}(\omega\underline{1}-\underline{K})^{-1}\underline{F}^{(0)}+$ c.c.	$C(2),C(3)$	$A(2),B(2),D(2),D(8),E(2),E(8)/$ $A(3),B(3),D(3),D(9),E(3),E(9)$
(III)	$\underline{F}^{(0)\dagger}(\omega\underline{1}-\underline{K})^{-1}\underline{C}^{(1)}(\omega\underline{1}-\underline{K})^{-1}\underline{C}^{(1)}(\omega\underline{1}-\underline{K})^{-1}\underline{F}^{(0)}$	$C(1)$ $X(5),X(11)/X(6),X(12),X=A,\ldots,E$ $Y(7)-Y(10),Y=A,B,C$ $Y(7)-Y(10),Y=A,B,C$	$A(1),B(1),D(1),D(7),E(1),E(7)$
(IV)/(IV)*	$\underline{F}^{(2)\dagger}(\omega\underline{1}-\underline{K})^{-1}\underline{F}^{(0)}+$ c.c.		
(V)	$\underline{F}^{(0)\dagger}(\omega\underline{1}-\underline{K})^{-1}\underline{C}^{(2)}(\omega\underline{1}-\underline{K})^{-1}\underline{F}(0)$		

FIG. 6. Second-order Goldstone diagrams (in Abrikosov notation) contributing to $\underline{\text{II}}_+$, the other 12 diagrams contributing to $\underline{\text{II}}_-$ are obtained by turning round these. The dotted lines indicate the external vertices.

tained from comparison of the contribution (III) with the six diagrams $A(1)$, $B(1)$, $D(1)$, $D(7)$, $E(1)$, and $E(7)$. Although a single diagram, say $A(1)$, contains terms which correspond to Pauli-forbidden configurations, e.g., $(ijkk)$, these terms cancel out if all six diagrams are taken into account. Thus, one may readily introduce the restriction $i < j$ and $k < l$ for the space of $2p$-$2h$ excitations $(ijkl)$. This also applies for the contribution (I) by which the modified transition moments $F_{ijkl}^{(1)}$ are obtained, as well as for the contributions (II) and (II)*. The latter contributions give no new information once $\underline{C}^{(1)}$ and $\underline{F}^{(1)}$ are determined; although, one does have to check that they are indeed consistent.

As has already been mentioned, there are 12 diagrams A, B, $C(7)$—(10) which do not fit as straightforwardly into the matrix scheme as the others. Each diagram has a cut corresponding to a $3p$-$3h$ denominator

$$(\omega + \epsilon_k + \epsilon_{k'} + \epsilon_s - \epsilon_j - \epsilon_{j'} - \epsilon_r)^{-1}$$

and one might conclude that this introduces an explicit coupling to the $3p$-$3h$ space. However, this is not the case, since these denominators are cancelled if one takes all four time orderings (7)—(10) for each species A, B, C into account. We shall demonstrate this for the diagrams $C(7)$—$C(10)$. The explicit contributions read

$$\sum_{I=7}^{10} C(I) = \sum_{\bar{n}_j n_k = \bar{n}_{j'} n_{k'} = 1} D_{jk}^* D_{j'k'} \sum_{r,s} V_{jr[ks]} V_{k's[j'r]} \bar{n}_r n_s h \ , \tag{49a}$$

where

$$h = \omega_{12}^{-1}(\omega_1^{-1}\omega_2^{-1} + \omega_1^{-1}\epsilon_1^{-1} + \omega_2^{-1}\epsilon_2^{-1} + \epsilon_1^{-1}\epsilon_2^{-1}) \tag{49b}$$

and

$$\omega_{12} = (\omega + \epsilon_k + \epsilon_{k'} + \epsilon_s - \epsilon_j - \epsilon_{j'} - \epsilon_r) ,$$

$$\omega_1 = (\omega + \epsilon_k - \epsilon_j) ,$$

$$\omega_2 = (\omega + \epsilon_{k'} - \epsilon_{j'}) , \tag{49c}$$

$$\epsilon_1 = (\epsilon_k + \epsilon_s - \epsilon_j - \epsilon_r) ,$$

$$\epsilon_2 = (\epsilon_{k'} + \epsilon_s - \epsilon_{j'} - \epsilon_r) .$$

The four energy-denominator products in h correspond to $C(7)$, $C(8)$, $C(9)$ and $C(10)$, respectively. As is apparent, h simplifies to

$$h = \omega_1^{-1}\omega_2^{-1}\epsilon_1^{-1}\epsilon_2^{-1}\tfrac{1}{2}\{\,\epsilon_1 + \epsilon_2 + \omega_1 + \omega_2\,\} = \omega_1^{-1}\omega_2^{-1}\frac{\tfrac{1}{2}(\epsilon_1 + \epsilon_2)}{\epsilon_1\epsilon_2} + \tfrac{1}{2}(\omega_1^{-1} + \omega_2^{-1})\frac{1}{\epsilon_1\epsilon_2} , \tag{50}$$

where the 3p-3h denominator ω_{12} is canceled. Inserting the last expression for h into the right-hand side of Eq. (49a) one obtains

$$\sum_{I=7}^{10} C(I) = \sum_{\substack{j,k \\ j',k'}} D_{jk}^* \frac{\widetilde{C}_{jk,j'k'}\bar{n}_j n_k \bar{n}_{j'} n_{k'}}{(\omega + \epsilon_k - \epsilon_j)(\omega + \epsilon_{k'} - \epsilon_{j'})} D_{j'k'} + \sum_{j,k} \frac{\bar{n}_j n_k}{\omega + \epsilon_k - \epsilon_j}(D_{jk}^* \widetilde{F}_{jk} + \widetilde{F}_{jk}^* D_{jk}) , \tag{51}$$

where

$$\widetilde{C}_{jk,j'k'} = \sum_{r,s} V_{jr[ks]}V_{k's[j'r]}\frac{\tfrac{1}{2}(\epsilon_k + \epsilon_{k'} - \epsilon_j - \epsilon_{j'}) + \epsilon_s - \epsilon_r}{(\epsilon_k + \epsilon_s - \epsilon_j - \epsilon_r)(\epsilon_{k'} + \epsilon_s - \epsilon_{j'} - \epsilon_r)}n_s\bar{n}_r \tag{52a}$$

$$\widetilde{F}_{jk} = \tfrac{1}{2}\sum_{\substack{r,s \\ j',k'}} \frac{V_{jr[ks]}V_{k's[j'r]}n_s\bar{n}_r\bar{n}_{j'}n_{k'}}{(\epsilon_k + \epsilon_s - \epsilon_j - \epsilon_r)(\epsilon_{k'} + \epsilon_s - \epsilon_{j'} - \epsilon_r)}D_{j'k'} . \tag{52b}$$

The first part on the right-hand side of Eq. (51) has the form of contribution (V) in Table I and $\widetilde{C}_{jk,j'k'}$ represents a contribution to $C_{jk,j'k'}^{(2)}$. The second part fits in contributions (IV) and (IV)* of Table I. Here, $\widetilde{F}_{jk}$ represents a contribution to the second-order modified transition matrix elements $\underline{F}^{(2)}$. By analogy, the diagrams A, $B(7)-(10)$ contribute to $\underline{C}^{(2)}$ and $\underline{F}^{(2)}$.

We now collect the final results $\underline{C}$ and $\underline{F}$ of the second-order scheme. The configuration space consists of all p-h excitations (j,k) and 2p-2h excitations (i,j,k,l) where the restriction $i < j$ and $k < l$ is maintained. The p-h interaction matrix elements $\underline{C}$ read

$$C_{jk,j'k'} = -V_{jk'[j'k]} + C_{jk,j'k'}^{(A)} + C_{jk,j'k'}^{(B)} + C_{jk,j'k'}^{(C)} ,$$

where

$$C_{jk,j'k'}^{(A)} = -\tfrac{1}{2}\sum_{ruv} V_{jr[uv]}V_{uv[j'r]}\bar{n}_r n_u n_v \frac{\epsilon_u + \epsilon_v - \epsilon_r - \tfrac{1}{2}(\epsilon_j + \epsilon_{j'})}{(\epsilon_u + \epsilon_v - \epsilon_r - \epsilon_j)(\epsilon_u + \epsilon_v - \epsilon_r - \epsilon_{j'})}\delta_{kk'} ,$$

$$C_{jk,j'k}^{(B)} = -\tfrac{1}{2}\sum_{urs} V_{rs[ku]}V_{k'u[rs]}n_u\bar{n}_r\bar{n}_s \frac{\tfrac{1}{2}(\epsilon_k + \epsilon_{k'}) + \epsilon_u - \epsilon_r - \epsilon_s}{(\epsilon_k + \epsilon_u - \epsilon_r - \epsilon_s)(\epsilon_{k'} + \epsilon_u - \epsilon_r - \epsilon_s)}\delta_{jj'} , \tag{53a}$$

$$C_{jk,j'k'}^{(C)} = \sum_{r,s} V_{jr[ks]}V_{k's[j'r]}\bar{n}_r n_s \frac{\tfrac{1}{2}(\epsilon_k + \epsilon_{k'} - \epsilon_j - \epsilon_{j'}) + \epsilon_s - \epsilon_r}{(\epsilon_k + \epsilon_s - \epsilon_j - \epsilon_r)(\epsilon_{k'} + \epsilon_s - \epsilon_{j'} - \epsilon_r)} .$$

Here, the superscripts A, B, and C indicate the origin of the respective contributions in the second-order diagrams. The p-h $-2p$-$2h$ coupling matrix elements read

$$C_{jk,i'j'k'l'} = \delta_{ji'} V_{k'l'[kj']} - \delta_{jj'} V_{k'l'[ki']} - \delta_{kk'} V_{jl'[i'j']} + \delta_{kl'} V_{jk'[i'j']} \, , \tag{53b}$$

and the $2p$-$2h$ interaction vanishes (in the strict second-order ADC)

$$C_{ijkl,i'j'k'l'} = 0 \, . \tag{53c}$$

The indices in these equations are restricted according to

$$\bar{n}_j n_k = \bar{n}_{j'} n_{k'} = \bar{n}_i \bar{n}_j n_k n_l = \bar{n}_{i'} \bar{n}_{j'} n_{k'} n_{l'} = 1 , \quad \text{and} \quad i < j \, , \ i' < j' \, , \ k < l, \ k' < l' \, .$$

The expression for the modified transition moments F_{jk} for the p-h space are somewhat lengthy, since the second-order contribution consists of 13 terms

$$F_{jk} = D_{jk} + \sum_{r,s} \frac{V_{js[rk]} \bar{n}_s n_r}{\epsilon_j + \epsilon_s - \epsilon_k - \epsilon_r} D_{rs} + F_{jk}^{(A)} + F_{jk}^{(B)} + F_{jk}^{(C)} + \sum_{I=1}^{10} F_{jk}^{(2,I)} \, , \quad \bar{n}_j n_k = 1 \, . \tag{54a}$$

The individual second-order contributions are listed in Appendix B. The modified transition moments F_{ijkl} for the $2p$-$2h$ space read

$$F_{ijkl} = \sum_v \left[\frac{V_{ij[vl]} n_v}{(\epsilon_v + \epsilon_l - \epsilon_i - \epsilon_j)} D_{vk} - \frac{V_{ij[vk]} n_v}{(\epsilon_k + \epsilon_v - \epsilon_i - \epsilon_j)} D_{vl} \right]$$

$$- \sum_s \left[\frac{V_{sj[kl]} \bar{n}_s}{\epsilon_k + \epsilon_l - \epsilon_j - \epsilon_s} D_{is} - \frac{V_{si[kl]} \bar{n}_s}{\epsilon_k + \epsilon_l - \epsilon_i - \epsilon_s} D_{js} \right] \, , \quad \bar{n}_i \bar{n}_j n_k n_l = 1 \, , \ i < j \, , \ k < l \, . \tag{54b}$$

The expressions (53) and (54) for $\underline{F}$ and $\underline{C}$ employed in the basic equation (48) define the second-order ADC scheme. Again, this approximation constitutes an infinite partial summation of the perturbation expansion of $T(\omega)$ being exact up to second order. A thorough discussion of the properties of this approximation is given in Sec. IV.

We mention, that it is straightforward extension to take into account the (first-order) $2p$-$2h$ interaction-matrix elements

$$C_{ijkl,i'j'k'l'} = \delta_{kk'} \delta_{ll'} V_{ij[i'j']} + \delta_{ii'} \delta_{jj'} V_{k'l'[kl]}$$

$$- \left[\delta_{jj'} \delta_{ll'} V_{ik'[i'k]} + \delta_{jj'} \delta_{kk'} V_{il'[i'l]} + \delta_{ii'} \delta_{ll'} V_{jk'[j'k]} + \delta_{ii'} \delta_{kk'} V_{jl'[j'l]} \right]$$

$$+ [k' \leftrightarrow l'] + [i' \leftrightarrow j'] - [k' \leftrightarrow l', i' \leftrightarrow j'] \, . \tag{55}$$

Thus an important class of third- (and higher-) order diagrams is included. As a result, the excitation energies for ($2h$-$2p$) excited states are obtained consistent through first order. This is discussed in Sec. IV.

We note that the equations (48), (53), (55), and (54) of the second-order ADC reflect the symmetry properties of the considered Hamiltonian $\hat{H}$ and

the transition operator $\hat{D}$, respectively. If, for instance, the Hamiltonian is spin independent, one easily arrives at a spin-free formulation for the diagonalization of the modified interaction matrix C, where singlet and triplet states are decoupled *a priori*.

IV. DISCUSSION OF THE FIRST- AND SECOND-ORDER ADC SCHEMES

Until now the discussion of the ADC scheme has concentrated upon formal aspects, but in order to obtain some physical insight it is useful to investigate the ADC approach within a wavefunction description for the ground and excited states. As a tool for this analysis we shall use the comparison with the lowest-order expressions of the familiar Rayleigh-Schrödinger perturbation theory for the excitation energies and transition moments. In addition, we shall compare the first- and second-order ADC with the TDA and RPA schemes. Both the RPA and the first-order ADC represent infinite partial summation for $T(\omega)$ [and $\underline{\Pi}(\omega)$] being exact up to first order. However, these methods achieve this result by a mathemati-

cally different procedure and it is interesting to demonstrate this difference explicitly. We start with a short presentation of the essential RPA and TDA equations in Sec IV A. A comparison of the second-order excitation energies is given in Sec. IV B. In Sec. IV C we consider the transition moments and in Sec. IV D we shortly discuss the ADC results for higher excited states.

A. The polarization propagator in the RPA and TDA

As is well known, there are many ways to derive the RPA-polarization propagator $\underline{\Pi}^{RPA}(\omega)$. Within our context one may start from the first-order Bethe-Salpeter equation which is obtained from Eq. (3) by replacing the full one-particle Green's functions G by free functions G^0 and the irreducible p-h vertex $K^{p\text{-}h}$ by its (constant) first-order contribution. Making use of Eq. (4) one arrives at the simple algebraic equation

$$\underline{\Pi}^{RPA}(\omega)=[\underline{\Pi}^{(0)^{-1}}(\omega)-\underline{C}^{RPA}]^{-1}\,,\tag{56}$$

where $\underline{\Pi}^{(0)}$ is the "free" polarization propagator

$$\Pi^{(0)}_{rs,r's'}(\omega)=\delta_{rr'}\delta_{ss'}\left[\frac{\bar{n}_r n_s}{\omega+\epsilon_s-\epsilon_r+i\eta}-\frac{n_r\bar{n}_s}{\omega+\epsilon_s-\epsilon_r-i\eta}\right]\tag{57}$$

and $\underline{C}^{RPA}$ is given by

$$C^{RPA}_{rs,r's'}=-V_{rs'[r's]}\,.\tag{58}$$

Here, the configurations space (r,s) comprises in addition to the p-h excitations, also the "unphysical" h-p excitations where r denotes a hole and s a particle state, respectively. Diagrammatically, the RPA polarization propagator represents the infinite partial summation of a special class of Feynman diagrams, namely, the RPA diagrams shown in Fig. 7. The first-order irreducible p-h vertex $\underline{C}^{RPA}$ of Eq. (58) is actually derived from the first-order diagram. By partitioning the matrix $\underline{C}^{RPA}$ into p-h and h-p parts one arrives at the familiar notation[14] for Eq. (56)

$$\underline{\Pi}^{RPA}(\omega)=\begin{bmatrix}\omega\underline{1}-\underline{K}-\underline{A} & -\underline{B}\\ -\underline{B}^* & -\omega\underline{1}-\underline{K}-\underline{A}^*\end{bmatrix}^{-1},$$

$$\tag{59a}$$

where

$$K_{jk,j'k'}=\delta_{jj'}\delta_{kk'}(\epsilon_j-\epsilon_k)\,,$$

$$A_{jk,j'k'}=-V_{jk'[j'k]}\,,$$

$$B_{jk,j'k'}=-V_{jj'[k'k]}\,,\tag{59b}$$

$$\bar{n}_j n_k=\bar{n}_{j'}n_{k'}=1\,.$$

As is well known, the matrix inversion problem according to Eq. (56) [or Eq. (59)] is equivalent to the RPA pseudoeigenvalue problem[14]
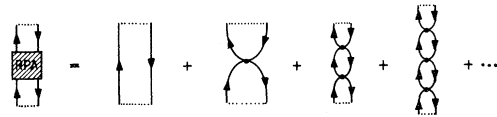
FIG. 7. Graphical representation of the RPA polarization propagator as a sum of Feynman diagrams.

$$(\underline{K} + \underline{C}^{\mathrm{RPA}})\underline{X} = \underline{N}\underline{X}\underline{\Omega}^{\mathrm{RPA}} \ , \tag{60a}$$

$$\underline{X}^{\dagger}\underline{N}\underline{X} = \underline{N} \ , \tag{60b}$$

where $\underline{X}$ and $\underline{\Omega}$ denote, respectively, the eigenvector matrix and the diagonal matrix of eigenvalues and $\underline{N}$ is a diagonal matrix,

$$N_{rs,r's'} = \delta_{rr'}\delta_{ss'}(\bar{n}_r n_s - n_r \bar{n}_s) \ . \tag{60c}$$

Similar to the exact polarization propagator, $\underline{\Pi}^{\mathrm{RPA}}$ is the sum of two equivalent parts [see Eqs. (7) and (8)]

$$\underline{\Pi}^{\mathrm{RPA}}(\omega) = \underline{\Pi}_{+}^{\mathrm{RPA}}(\omega) + \underline{\Pi}_{-}^{\mathrm{RPA}}(\omega) \ . \tag{61}$$

According to Eq. (16), the RPA-transition function is given by

$$T^{\mathrm{RPA}}(\omega) = \underline{D}^{\dagger}\underline{\Pi}_{+}^{\mathrm{RPA}}(\omega)\underline{D} \ . \tag{62}$$

The TDA results by restricting the RPA equations (59) and (62) to the p-h space:

$$\underline{\Pi}^{\mathrm{TDA}}(\omega) = (\omega\underline{1} - \underline{K} - \underline{A})^{-1} \ , \tag{63}$$

$$T^{\mathrm{TDA}}(\omega) = \underline{D}^{\dagger}\underline{\Pi}^{\mathrm{TDA}}(\omega)\underline{D} \ . \tag{64}$$

Clearly, Eq. (63) represents a Hermitian eigenvalue problem within the space of p-h excitations. Diagrammatically, the TDA-polarization propagator of Eq. (63) represents the infinite sum of certain Goldstone diagrams, namely, the first time-ordered Goldstone diagram associated with each RPA-Feynman diagram of Fig. 7.

B. Particle-hole excitation energies up to second-order perturbation theory

We consider an (singly) excited state $|\Psi_{ab}\rangle$ which derives (in the sense of the adiabatic theorem) from the unperturbed singly excited configuration (p-h excitation)

$$|\Phi_{ab}\rangle = c_a^{\dagger}c_b |\Phi_0\rangle \ . \tag{65}$$

Here, $|\Phi_0\rangle$ denotes the Hartree-Fock ground state. The exact ground-state energy up to second order $E_0(2)$ is given by the familiar Rayleigh-Schrödinger expression

$$E_0(2) = E_0(1)$$
$$- \sum_{\substack{i<j \\ k<l}} \frac{|V_{ij[kl]}|^2}{\epsilon_i + \epsilon_j - \epsilon_k - \epsilon_l} \bar{n}_i \bar{n}_j n_k n_l \ , \tag{66}$$

where

$$E_0(1) = \langle \Phi_0 | H | \Phi_0 \rangle \tag{67}$$

is the first-order ground-state energy. The energy of the excited state up to second order reads

$$E_{ab}(2) = E_0(1) + \epsilon_a - \epsilon_b - V_{ab[ab]} + U_{ab}(p\text{-}h) + U_{ab}(2p\text{-}2h) + U_{ab}(3p\text{-}3h) \ . \tag{68a}$$

Here, the three terms $U_{ab}(np\text{-}nh)$, $n = 1,2,3$ denote second-order contributions arising, from the interaction of the configuration $|\Phi_{ab}\rangle$ with (other) p-h, $2p$-$2h$, and $3p$-$3h$ excitations, respectively:

$$U_{ab}(p\text{-}h) = \sum_{\substack{j,k \\ \neq (a,b)}} \frac{|V_{ak[bj]}|^2}{\epsilon_a - \epsilon_b - \epsilon_j + \epsilon_k} \bar{n}_j n_k \ , \tag{68b}$$

$$U_{ab}(2p\text{-}2h) = \sum_{\substack{j\neq a \\ k<l}} \frac{|V_{bj[kl]}|^2 \bar{n}_j n_k n_l}{-\epsilon_b - \epsilon_j + \epsilon_k + \epsilon_l} + \sum_{\substack{i<j' \\ k\neq b}} \frac{|V_{ak[ij]}|^2 \bar{n}_i \bar{n}_j n_k}{\epsilon_a + \epsilon_k - \epsilon_i - \epsilon_j} + \left[\sum_{\substack{j\neq a \\ k\neq b}} \frac{V_{aj[ak]}V_{bj[bk]}^*}{\epsilon_j - \epsilon_k} \bar{n}_j n_k + \text{c.c.} \right] \ , \tag{68c}$$

$$U_{ab}(3p\text{-}3h) = - \sum_{\substack{i<j\neq a \\ k<l\neq b}} \frac{|V_{ij[kl]}|^2}{\epsilon_i + \epsilon_j - \epsilon_k - \epsilon_l} \bar{n}_i \bar{n}_j n_k n_l \ . \tag{68d}$$

Now the second-order excitation energy ΔE_{ab} is easily obtained by subtracting Eq. (66) from Eq. (68a):

$$\Delta E_{ab} = E_{ab}(2) - E_0(2) = \epsilon_a - \epsilon_b - V_{ab[ab]} + U_{ab}(p\text{-}h) + U_{ab}(2p\text{-}2h) + R_{ab} \ , \tag{69a}$$

where

$$R_{ab} = \sum_{j,k<l} \frac{|V_{aj[kl]}|^2 \bar{n}_j n_k n_l}{\epsilon_a + \epsilon_j - \epsilon_k - \epsilon_l} + \sum_{k,i<j} \frac{|V_{ij[bk]}|^2 \bar{n}_i \bar{n}_j n_k}{\epsilon_i + \epsilon_j - \epsilon_k - \epsilon_b} - \sum_{j,k} \frac{|V_{aj[kb]}|^2 \bar{n}_j n_k}{\epsilon_a + \epsilon_j - \epsilon_b - \epsilon_k} \tag{69b}$$

is the remainder of a partial cancelation of the $3p$-$3h$ contribution $U_{ab}(3p\text{-}3h)$ for the excited states and the $2p$-$2h$ contribution for the ground state.

Now we are in the position to compare the second-order excitation energies with the second-order expressions resulting from the ADC schemes, the TDA, and the RPA. We begin with the second-order ADC as defined by Eqs. (48), and (53)—(55). Here, by construction, the excitation energies are exact up to second order, i.e., given by Eq. (69). It is interesting to trace the different contributions within the algebraic scheme. The straightforward matrix-perturbation theory identifies the first-order contribution on the right-hand side of Eq. (69) as the diagonal matrix element of $\underline{K}$ and $\underline{C}^{(1)}$:

$$\epsilon_a - \epsilon_b - V_{ab[ab]} = K_{ab,ab} + C^{(1)}_{ab,ab} \ . \tag{70}$$

The part $U_{ab}(p\text{-}h)$ is associated with the interaction of $|\Phi_{ab}\rangle$ with the other p-h excitations $(j,k) \neq (a,b)$ and $U_{ab}(2p\text{-}2h)$ results from the interaction with the $2p$-$2h$ excitations according to the matrix elements (53b). The interesting part R_{ab} of Eq. (70b) corresponds to the second-order diagonal matrix element

$$R_{ab} = C^{(2)}_{ab,ab} \ . \tag{71}$$

As has been discussed above, $\underline{C}^{(2)}$ is derived diagrammatically from the time orderings (7)—(10) of the diagrams A, B, and C of Fig. 6. One may easily check that the three parts of R_{ab} in Eq. (69b) correspond to the individual contributions of diagram A, B, and C, respectively.

As we have seen, the second-order Rayleigh-Schrödinger expression (69) for the excitation energies includes contributions associated with doubly excited $(2p$-$2h)$ configurations in the ground-state wave function and with triply excited $(3p$-$3h)$ configurations in the wave function of the excited state. This means that, within a wave-function approach, e.g., the conventional configuration interaction (CI), one has to perform a double excitation CI calculation for the ground state and a triple excitation CI calculation for the excited states in order to obtain the $(p$-$h)$ excitation energies consistent through second order. The polarization

propagator calculation by the second-order ADC scheme, on the other hand, achieves its result by one diagonalization within the space of singly $(p$-$h)$ and doubly $(2p$-$2h)$ excited configurations. Here, the modified p-h-interaction matrix elements $\underline{C}^{(2)}$ account for the second-order ground-state correlation and the interaction with the triply excited configurations.

We now turn to a discussion of the TDA and RPA results. The second-order excitation energies within the TDA approach are found to be

$$\Delta E_{ab}^{TDA} = \epsilon_a - \epsilon_b - V_{ab[ab]} + U_{ab}(p\text{-}h) \ . \tag{72}$$

Obviously, this expression is only exact up to first order, since in second order only the interaction of the special p-h excitation (a,b) with the other p-h excitations is taken into account.

For the RPA, we find by a straightforward perturbation theory for Eq. (60) the second-order result

$$\Delta E_{ab}^{RPA} = \epsilon_a - \epsilon_b - V_{ab[ab]} + U_{ab}(p\text{-}h)$$
$$- \sum_{j,k} \frac{|V_{aj[kb]}|^2 \bar{n}_j n_k}{\epsilon_a + \epsilon_j - \epsilon_b - \epsilon_k} \ . \tag{73}$$

By comparing with the full second-order expression (69) one immediately sees that the RPA excitation energies are only exact up to first order. As the TDA, the contribution $U_{ab}(2p\text{-}2h)$ of the $2p$-$2h$ excitations for the excited state is completely absent. Since this contribution represents a significant reduction of the energies of the excited states, the RPA (and TDA) excitation energies are, in general, too large. The contribution R_{ab} of Eq. (69b) is only partly considered by the RPA. Only the third term corresponding to the RPA diagrams $C(7)-C(10)$ is taken into account. Consequently, the RPA excitation energies might only be better than the TDA results because of accidental numerical compensation, and, in fact, are often not as good. This can be seen by inspection of the full contribution R_{ab} of Eq. (69b): whereas the first two parts corresponding to diagram A, $B(7-10)$ which are missing in the RPA, are positive, the third part, included in the RPA, is negative. Thus, the RPA always lowers the TDA excitation ener-

gies (in second order), whereas the full correction R_{ab} in general is positive. In contrast to what is often assumed, the RPA should by no means be more highly esteemed than the TDA, at least as far as the excitation energies of finite Fermi systems are concerned. On the other hand, the RPA is superior to the TDA with respect to the transition moments which are calculated consistent through first order by the RPA as will be discussed in Sec. IV C.

C. Transition moments up to first-order perturbation theory

Now we consider the transition moment

$$T_{ab} = \langle \Psi_{ab} \mid \hat{D} \mid \Psi_0 \rangle \qquad (74)$$

for the $(p\text{-}h)$ excited state $\mid \Psi_{ab} \rangle$. Here, $\hat{D}$ is the one-particle transition operator of Eq. (10). Up to first order one obtains

$$T_{ab}^{(1)} = \langle \Phi_{ab} \mid \hat{D} \mid \Phi_0 \rangle + \langle \Phi_{ab} \mid \hat{D} \mid \Psi_0^{(1)} \rangle$$
$$+ \langle \Psi_{ab}^{(1)} \mid \hat{D} \mid \Phi_0 \rangle , \qquad (75\text{a})$$

$$\langle \Phi_{ab} \mid \hat{D} \mid \Phi_0 \rangle = D_{ab} , \qquad (75\text{b})$$

$$\langle \Phi_{ab} \mid \hat{D} \mid \Psi_0^{(1)} \rangle = \sum_{jk} \frac{V_{aj[kb]} \bar{n}_j n_k}{\epsilon_a + \epsilon_j - \epsilon_b - \epsilon_k} D_{kj} , \qquad (75\text{c})$$

$$\langle \Psi_{ab}^{(1)} \mid \hat{D} \mid \Phi_0 \rangle = \sum_{j,k \neq (a,b)} \frac{V_{ak[bj]} \bar{n}_j n_k}{\epsilon_a - \epsilon_j - \epsilon_b + \epsilon_k} D_{jk} . \qquad (75\text{d})$$

The first term (75b) is the zeroth-order transition moment. The two first-order contributions (75c) and (75d) correspond to the first-order ground state and to the first-order excited state, respectively. We note that only the singly $(p\text{-}h)$ excited configurations in $\mid \Psi_{ab}^{(1)} \rangle$ give a contribution to $T_{ab}^{(1)}$.

As in Sec. IV B, we now compare the first-order transition moments with the outcome of the TDA, RPA, and ADC. For the TDA we find

$$T_{ab}^{\text{TDA}} = \underline{X}_{ab}^{\dagger} \underline{D} , \qquad (76)$$

where $\underline{X}_{ab}$ denotes the eigenvector associated with the excited state $\mid \Psi_{ab}^{\text{TDA}} \rangle$. Up to first order its elements read

$$X_{jk,ab}^{(0)} = \begin{cases} 1 & \text{for } j = a, \ k = b \\ 0 & \text{else} \end{cases} \qquad (77\text{a})$$

$$X_{jk,ab}^{(1)} = \begin{cases} 0 & \text{for } j = a , \ k = b \\ \dfrac{V_{bj[ak]}}{\epsilon_a - \epsilon_j - \epsilon_b + \epsilon_k} & \text{else, } \bar{n}_j n_k = 1 . \end{cases} \qquad (77\text{b})$$

Inserting these results into the right-hand side of Eq. (76) one immediately sees that T_{ab}^{TDA} comprises the first and the third term of the full first-order transition moment T_{ab}, whereas the ground-state correlation term (75c) is missing.

The RPA, on the other hand, renders the transition moments exact up to first order. By partitioning the RPA eigenvector corresponding to the $p\text{-}h$ excited state $\mid \Psi_{ab} \rangle$ into a $p\text{-}h$ part $\underline{X}_{ab}$ and into a $h\text{-}p$ part $\underline{Y}_{ab}$ one may write

$$T_{ab}^{\text{RPA}} = (\underline{X}_{ab}^{\dagger} \underline{Y}_{ab}^{\dagger}) \underline{D} , \qquad (78)$$

where, of course, the vector $\underline{D}$ now comprises the $h\text{-}p$ part as well. The contributions up to first order for the $p\text{-}h$ part $\underline{X}_{ab}$ are identical with the TDA results of Eq. (77), while for the $h\text{-}p$ part one finds up to first order

$$Y_{jk,ab} = \frac{V_{kb[aj]}}{\epsilon_a + \epsilon_j - \epsilon_k - \epsilon_b} , \quad \bar{n}_j n_k = 1 . \qquad (79)$$

Clearly, by inserting the first-order results for $\underline{X}_{ab}$ and $\underline{Y}_{ab}$ in the expressions on the right-hand side of Eq. (78), one recovers the full first-order contribution of T_{ab}. Thus, one can say that the RPA provides both the transition energies and moments exact up to first order, whereas the TDA gives exact first-order results only for the transition energies. In particular, the inclusion of the first-order ground-state correlation term for the transition moment justifies the common statement that the RPA, in contrast to the TDA, considers ground-state correlation.

Finally, we consider the ADC result. By construction the first-order ADC defined by Eqs. (41) and (45) already gives the full first-order transition moment. As has been mentioned above, the eigenvalue problem of the first-order ADC is identical with the TDA problem. This can be seen by inspection of the Eqs. (41), (45), (59) and (63). Correspondingly, the eigenvector $\underline{X}_{ab}$ for the $p\text{-}h$ excited state $\mid \Psi_{ab} \rangle$ is identical to the TDA eigenvector. For the ADC, however, the transition moment is obtained by multiplying $\underline{X}_{ab}$ with the vector $\underline{F}$ of the modified transition matrix elements of Eq. (45b):

$$T_{ab}^{\text{ADC}} = \underline{X}_{ab}^{\dagger} \underline{F} . \qquad (80)$$

Up to first order this yields

$$T_{ab}^{\text{ADC}}(1) = \underline{X}_{ab}^{(0)\dagger} \underline{F}^{(0)} + \underline{X}_{ab}^{(0)\dagger} \underline{F}^{(1)} + \underline{X}_{ab}^{(1)\dagger} \underline{F}^{(0)} , \qquad (81)$$

in accordance with the three terms of the first-order transition moment given in Eq. (75).

We have seen that the RPA can be viewed as an infinite partial summation for the polarization propagator, which is exact up to first order both for the $(p\text{-}h)$ excitation energies and the transition moments. This also applies for the first-order ADC scheme. However, both methods are quite distinct and it is worthwhile to repeat the differences in the mathematical procedures. The RPA represents a non-Hermitian (pseudo) eigenvalue problem in a configuration space, which is twice as large as the space of the singly $(p\text{-}h)$ excited configurations. The RPA transition moments are obtained by multiplying the RPA eigenvectors by the original transition-matrix elements D_{rs} [Eq. (78)]. The first-order ADC scheme, on the other hand, is (as the TDA) a Hermitian eigenvalue in the space of singly excited configurations. Instead of using the matrix elements of $\hat{D}$, one multiplies the eigenvectors with modified transition-matrix elements $\underline{F}$ in order to obtain the transition moments.

Similarly, one can analyze the second-order contributions for the transition moments. However, since the resulting expressions are already somewhat lengthy, we do not enter this discussion here. We only mention that, again, the second-order ADC scheme of Eqs. (48), (53), and (54) gives the correct second-order results, whereas the RPA results are already incomplete and selective in this order.

D. Higher excited states

In Sec. IV B and Sec. IV C we have discussed the excitation energies and transition moments of excited states which derive (in the sense of the adiabatic theorem) from the unperturbed singly excited $(p\text{-}h)$ configurations. These states may be called the main states of the spectrum associated with the transition operator $\hat{D}$. Here, already the zeroth-order transition moments contribute to the spectral strength. In addition to the main states, there occur secondary states in the spectrum which are related to higher excited configurations, e.g., the doubly excited $(2p\text{-}2h)$ configurations

$$| \Phi_{ijkl} \rangle = c_i^\dagger c_j^\dagger c_k c_l | \Phi_0 \rangle ,$$
$$\bar{n}_i \bar{n}_j n_k n_l = 1 . \tag{82}$$

We note that the zeroth-order transition moments $\langle \Phi_{ijkl} | \hat{D} | \Phi_0 \rangle$ vanish (as long as $\hat{D}$ is a one-particle operator).

In the first-order ADC scheme, as in the TDA and RPA, higher excited states are not considered at all. In the second-order ADC scheme the doubly excited $(2p\text{-}2h)$ configurations of Eq. (82) come into play. Of course, the resulting $(2p\text{-}2h)$ excited states cannot be expected to be consistent through second order. For these states, the consistency of the transition function $T(\omega)$ through second order implies that the transition moments and excitation energies are consistent through first and zeroth order, respectively. As has already been mentioned, a simple extension of the strict second-order ADC scheme, namely, the consideration of the $2p\text{-}2h$ interaction-matrix elements (55), yields also the excitation energies exact up to first order. The correct first-order expressions read

$$\Delta E_{ijkl} = \epsilon_i + \epsilon_j - \epsilon_k - \epsilon_l + C_{ijkl,ijkl} , \tag{83}$$

where $C_{ijkl,ijkl}$ is given by Eq. (55).

We finally consider the transition moments for the higher excited states. The perturbation expansion of the $2p\text{-}2h$ excited state $| \Psi_{ijkl} \rangle$ deriving from $| \Phi_{ijkl} \rangle$ up to first order reads

$$| \Psi_{ijkl} \rangle = | \Phi_{ijkl} \rangle - \frac{V_{kl[ij]}}{\epsilon_i + \epsilon_j - \epsilon_k - \epsilon_l} | \Phi_0 \rangle$$

$$+ | p\text{-}h \rangle + | 2p\text{-}2h \rangle + | 3p\text{-}3h \rangle$$

$$+ | 4p\text{-}4h \rangle . \tag{84}$$

The contributions $| np\text{-}nh \rangle$ $(n = 1,2,3,4)$ arising from the (linear) coupling of the doubly excited $(2p\text{-}2h)$ configuration $| \Phi_{ijkl} \rangle$ with $np\text{-}nh$ excitations are somewhat lengthy and need not be specified here. The transition moment

$$T_{ijkl} = \langle \Psi_{ijkl} | \hat{D} | \Psi_0 \rangle \tag{85}$$

obviously has no zeroth-order contribution for a single-particle operator $\hat{D}$. The first nonvanishing term occurs in first order

$$T_{ijkl}^{(1)} = \langle \Phi_{ijkl} | \hat{D} | \Psi_0^{(1)} \rangle + \langle \Psi_{ijkl}^{(1)} | \hat{D} | \Phi_0 \rangle . \tag{86}$$

For $| \Psi_{ijkl}^{(1)} \rangle$ in the second term the $np\text{-}nh$ excitations with $n \geq 2$ make no contribution, accordingly, we obtain

$$T_{ijkl}^{(1)} = \langle \Phi_{ijkl} | \hat{D} | \Psi_0^{(1)} \rangle$$

$$- \frac{V_{ij[kl]}}{\epsilon_i + \epsilon_j - \epsilon_k - \epsilon_l} \langle \Phi_0 | \hat{D} | \Phi_0 \rangle$$

$$+ \langle p\text{-}h | \hat{D} | \Phi_0 \rangle . \tag{87}$$

The first two terms are readily identified with the modified transition-matrix elements of Eq. (54b)

$$F_{ijkl}^{(1)} = \langle \Phi_{ijkl} | \hat{D} | \Psi_0^{(1)} \rangle$$

$$- \frac{V_{ij[kl]}}{\epsilon_i + \epsilon_j - \epsilon_k - \epsilon_l} \langle \Phi_0 | \hat{D} | \Phi_0 \rangle . \tag{88}$$

The remaining term $\langle \mathrm{ph} | \hat{D} | \Phi_0 \rangle$, associated with the singly excited $(p\text{-}h)$ configurations in the excited state $| \Psi_{ijkl} \rangle$, is included in the ADC according to the interaction-matrix elements (53b).

V. CONCLUSIONS

The algebraic diagrammatic construction (ADC) presented in this article allows the summation of the diagrammatic perturbation expansion of the transition function $T(\omega)$. This function, being (for a general transiton operator) equivalent to the polarization propagator, can be written in the useful form of Eqs. (25) which in turn splits the problem of determining $T(\omega)$ into two separate problems, namely, the construction of the modified transition moments $\underline{F}$, and the diagonalization problem for the modified interaction matrix $\underline{C}$.

The general ADC scheme introduces in a natural way its nth order approximations representing infinite partial summations exact up to nth order. The zeroth-, first-, and second-order ADC schemes have been explicitly constructed and discussed. We wish to repeat here the main features of these schemes. First we stress that the mathematical procedure requires the solution of a Hermitian eigenvalue problem for a restricted space of unperturbed excited configurations (physical excitations). This is an important advantage with respect to RPA-like approximations, which encounter a non-Hermitian eigenvalue problem and, in general, deal with undesirably large configuration spaces, since unphysical excitations have to be included. The ADC, on the other hand, introduces modified matrix elements (and transition moments) which are no longer first-order (zeroth-order) expressions in the two-particle interaction, but include higher-order terms which are derived from the diagrammatic perturbation theory. Thus, the ADC may be viewed as representing an advantageous *mixtum compositum* of a diagonalization problem and perturbation theory.

The first-order ADC is formulated within the space of the $p\text{-}h$ excitations. The diagonalization problem, yielding the excitation energies, is equivalent to the TDA scheme. In contrast to the

TDA, however, the resulting eigenvectors are multiplied by modified transition-matrix elements; consequently both the excitation energies and the transition moments are consistent through first order, as has been shown by analyzing the results using formal perturbation theory. In this sense the first-order ADC is analogous to the RPA which also gives results consistent through first order. We would also note that the RPA has some obvious deficiencies which are avoided in the first-order ADC, e.g., selective and unbalanced contributions in second and higher order and the occurrence of complex solutions for excitation energies of low-lying excited states.

A decisive step beyond the RPA is certainly the second-order ADC scheme: its configuration space comprises the $p\text{-}h$ and $2p\text{-}2h$ excitations, and is thus of a size, which is familiar from the conventional CI calculations. The modified interaction-matrix elements and the modified transition moments contain terms of second order in the interaction, however, the expressions given by Eqs. (53) and (54) are still quite transparent and easy to implement in a computer program. By construction, the excitation energies and the transition moments of the singly excited states are now exact up to second order. We emphasize once more that in order to be consistent through second order in a wave-function approach one has to take into account already $3p\text{-}3h$ excitations (triply excited configurations with respect to the HF ground state) for the excited states and $2p\text{-}2h$ excitations for the ground state. In addition to the main excited states connected with the $p\text{-}h$ excitations, higher excited $(2p\text{-}2h)$ states are obtained in the second-order ADC, being consistently treated through first order. We believe that the second-order ADC scheme, in particular, will prove to be a successful approximation scheme for the excitation problem, maintaining the advantages of the many-body approach, i.e., the direct and consistent calculation of the transition energies and moments, and circumventing the difficulties and complexities of the previous RPA-like approximations.

APPENDIX A

Diagrammatic rules

In the following we briefly review the rules for the diagrammatic perturbation expansion of the polarization propagator and the transition function. We start with the rules for the Feynman diagrams (for more details see, e.g., Fetter and Walecka[6]).

(F1) Draw all topologically distinct connected diagrams with n interaction (wavy) lines and $2n + 2$ directed free Green's function (solid) lines, which start and end at the external times t' and t, respectively, with a pair of up- and downwards-directed free Green's functions.

(F2) Skip all disjoint graphs, i.e., graphs of the structure shown in Fig. 1. Such terms are exactly canceled by the second part on the right-hand side of Eq. (20).

(F3) Label the graphs with one-particle indices and time arguments according to Fig. 3. This figure also defines the graphical symbols. Sum over all internal indices and integrate over all internal times.

(F4) Multiply by a sign factor $(-1)^L$, where L is the number of closed (fermion) loops and by an additional factor $(+i)$ stemming from the definition (20). When all i factors for the nth order diagram are collected one obtains the overall factor

$$(+i)(-i)^n(i)^{2n+2} = -(i)^{n+1} .$$

Employing the Abrikosov notation, i.e., replacing the wavy interaction lines by interaction points representing the antisymmetrized matrix elements

$$V_{ij[kl]} = V_{ijkl} - V_{ijlk} ,$$

reduces the number of diagrams considerably, although, the overall sign is not uniquely determined in this notation.

(F5) The correct sign of the graph follows from the comparison with the sign of one Feynman graph which is contained in the Abrikosov graph.

(F6) As an additional rule for Abrikosov graphs one has to multiply each graph by 2^{-P}, where P is the number of permutations of two G^0 lines leaving the graph topologically unchanged.

As an example we consider the second-order Feynman diagram A, represented by the graph $A(1)$ in Fig. 5

$$A(t,t') = i^3 \frac{1}{2} \sum_{r,s,n} V_{jn[rs]} V_{rs[j'n]} \, G_k^0(t',t) \int_{-\infty}^{\infty} \int_{-\infty}^{\infty} dt_1 \, dt_2 G_j^0(t,t_1) G_r^0(t_1,t_2) G_s^0(t_1,t_2) G_n^0(t_2,t_1) G_{j'}^0(t_2,t') . \quad \text{(A1)}$$

Here one finds $L = 1$ and $P = 1$.

The evaluation of an nth order Feynman diagram $X(t,t')$ requires the performance of n time integrations over the internal time indices $t_1' \ldots t_n$. The result of these integrations and of the additional Fourier transformation

$$X(\omega) = \int_{-\infty}^{\infty} e^{i\omega(t-t')} X(t,t') d(t-t') \quad \text{(A2)}$$

can be read directly off the so-called Goldstone diagrams. The rules to draw and evaluate the Goldstone diagrams are as follows:

(G1) For a given nth order Feynman diagram, draw all $(n + 2)!$ time-ordered diagrams which result from permuting the ordering of the times $t, t_1' \ldots t_n, t'$. For definitness, we refer to a representation of the Feynman diagrams where t and t' are the upper and lower external times, respectively, and where the pairs of external lines are ordered such that the first line is directed upwards and the second line is directed downwards (see the examples in Figs. 5 and 6). We further introduce an auxiliary line connecting the external times t and t' with the direction $t \rightarrow t'$.

(G2) For the Goldstone diagrams the direction of the lines has a meaning: Upwards- and downwards-directed lines represent particles (unoccupied one-particle states) and holes (occupied one-particle states), respectively. Label all lines with one-particle indices respecting this distinction.

(G3) There are no longer time arguments associated with each vertex. Instead, each cut (a horizontal line) between two successive vertices (including the external) introduces a denominator of the type

$$(\sigma\omega + \epsilon_k + \epsilon_l \ldots - \epsilon_i - \epsilon_j - \ldots + i\eta)^{-1} .$$

Here, each cut line gives a contribution: hole-lines $k, l, \ldots$, contribute the one-particle energies ϵ_k, $\epsilon_l, \ldots$; particle line $i, j, \ldots$, contributes the negative energies $-\epsilon_i$, $-\epsilon_j, \ldots$. The energy variable ω is introduced if the auxiliary line is cut, and has a positive $(\sigma = 1)$ or a negative sign $(\sigma = -1)$ according to the downward or upward direction, respec-

tively. If the auxiliary line is not cut, then $\sigma=0$ and a constant denominator results in which the imaginary infinitesimal $i\eta$ can be omitted.

(G4) Each hole line introduces the factor (-1). Thus, multiply by a sign factor $(-1)^{L+M}$, where L is the number of closed loops and M is the number of hole lines. Since each interaction vertex gives a factor $(-i)$ and each cut gives a factor $(+i)$, one obtains together with the factor $+i$ from the defin-

ition (20) the additional overall factor $(+i)$ $(-i)^n$ $\times (i)^{n+1}=-1$.

For the Goldstone diagrams one may also employ the Abrikosov notation; the corresponding rules (G5) and (G6) are analogous to (F5) and (F6). As an example we consider the second-order Gold-stone diagram $A(8)$ of Fig. 5:

$$A(8)=-\tfrac{1}{2}\sum_{ruv}V_{jr[uv]}V_{uv[j'r]}\bar{n}_r n_u n_v(\omega+\epsilon_k-\epsilon_{j'}+i\eta)^{-1}(\omega+\epsilon_k+\epsilon_u+\epsilon_v-\epsilon_j-\epsilon_r+i\eta)^{-1}(\epsilon_u+\epsilon_v-\epsilon_{j'}-\epsilon_r)^{-1}.$$

$$\text{(A3)}$$

Here, $M=3$, $L=1$, $P=1$.

The $(n+2)!$ Goldstone diagrams of a given nth order Feynman diagram can be divided into two classes of diagrams according to the two possibilities $t<t'$ and $t'<t$ for the external vertices. As is clear from the rule (G3), the diagrams of the first class have only $+i\eta$ denominators (analytic in the upper half of the complex plane) and contribute exclusively to the part $\underline{\Pi}_+$ of the polarization propagator. Analogously, the second class contributes only to $\underline{\Pi}_-$.

The transition function $T(\omega)$ [defined by Eq. (16)] derives from part $\underline{\Pi}_+$ of the polarization propagator. Each diagram for $\underline{\Pi}_+$ corresponds to a diagram for $T(\omega)$ by associating the transition-matrix elements D_{rs} with the external vertices. To be definite, one may start from the original Feynman diagram with the upper vertex D_{jk}^* and the lower vertex $D_{j'k'}$. As examples we refer to the diagrams $C(7)-C(10)$ of Fig. 5 which yield the contributions in Eq. (49). Finally, it is worth mentioning that an explicit expression for the full second-order contribution of $T(\omega)$ [and $\underline{\Pi}_+(\omega)$] is readily obtained by using the expressions (53) and (54) in the algebraic terms collected in Table I.

APPENDIX B

Second-order terms of the modified transition momnets for the p-h space

Here we present the explicit expressions of the second-order terms appearing on the right-hand side of Eq. (54a). The first three terms correspond to the time orderings $(7)-(10)$ of the diagram types A, B, and C, respectively. The following ten terms $F_{jk}^{(2,I)}$, $I=1,\ldots,10$ correspond to the time orderings $(5)/(6)$ and $(11)/(12)$ of the diagram types $A-E$:

$$F_{jk}^{(A)}=-\tfrac{1}{4}\sum\frac{V_{jr[nv]}V_{nv[sr]}}{\epsilon[nvrj]\epsilon[nvrs]}D_{sk}\,,\qquad\text{(B1)}$$

$$F_{jk}^{(B)}=-\tfrac{1}{4}\sum\frac{V_{rs[kn]}V_{vn[rs]}}{\epsilon[knrs]\epsilon[nvrs]}D_{jv}\,,\qquad\text{(B2)}$$

$$F_{jk}^{(C)}=\tfrac{1}{2}\sum\frac{V_{jr[kn]}V_{vn[sr]}}{\epsilon[knjr]\epsilon[vnsr]}D_{sv}\,,\qquad\text{(B3)}$$

$$F_{jk}^{(2,1)}=-\tfrac{1}{2}\sum\frac{V_{rs[nv]}V_{nj[rs]}}{\epsilon[vj]\epsilon[nvrs]}D_{vk}\,,\qquad\text{(B4)}$$

$$F_{jk}^{(2,2)}=\tfrac{1}{2}\sum\frac{V_{nv[rw]}V_{rj[nv]}}{\epsilon[wj]\epsilon[nvrj]}D_{wk}\,,\qquad\text{(B5)}$$

$$F_{jk}^{(2,3)}=-\tfrac{1}{2}\sum\frac{V_{rs[nv]}V_{nv[ks]}}{\epsilon[kr]\epsilon[nvrs]}D_{jr}\,,\qquad\text{(B6)}$$

$$F_{jk}^{(2,4)}=\tfrac{1}{2}\sum\frac{V_{rs[kn]}V_{tn[rs]}}{\epsilon[kt]\epsilon[knrs]}D_{jt}\,,\qquad\text{(B7)}$$

$$F_{jk}^{(2,5)}=\sum\frac{V_{jn[rk]}V_{rs[vn]}}{\epsilon[kvjs]\epsilon[nvrs]}D_{vs}\,,\qquad\text{(B8)}$$

$$F_{jk}^{(2,6)}=\sum\frac{V_{ns[vr]}V_{jr[nk]}}{\epsilon[knjr]\epsilon[kvjs]}D_{vs}\,,\qquad\text{(B9)}$$

$$F_{jk}^{(2,7)}=-\sum\frac{V_{jv[ns]}V_{sr[vk]}}{\epsilon[knjr]\epsilon[kvrs]}D_{nr}\,,\qquad\text{(B10)}$$

$$F_{jk}^{(2,8)}=-\sum\frac{V_{js[vn]}V_{nr[sk]}}{\epsilon[kvjr]\epsilon[nvjs]}D_{vr}\,,\qquad\text{(B11)}$$

$$F_{jk}^{(2,9)}=-\sum\frac{V_{jr[st]}V_{st[nk]}}{\epsilon[knjr]\epsilon[knst]}D_{nr}\,,\qquad\text{(B12)}$$

$$F_{jk}^{(2,10)}=-\tfrac{1}{2}\sum\frac{V_{jr[vw]}V_{vw[nk]}}{\epsilon[knjr]\epsilon[vwjr]}D_{nr}\,.\qquad\text{(B13)}$$

Here, the summations run over all occuring indices except j and k. We use the convention that r, s, t denote particles (unoccupied one-particle states) and n, v, w denote holes (occupied one-particle states). The symbol $\epsilon[nv\ldots rs\ldots]$ denotes the sum

$$\epsilon[nv\ldots rs\ldots]=\epsilon_n+\epsilon_v+\ldots-\epsilon_r-\epsilon_s-\ldots$$

of one-particle energies.

[1]An introduction can be found in various textbooks and monographs. Besides Refs. 2−6, and 18 we mention R. D. Mattuck, *A Guide to Feynmann Diagrams in the Many-Body Problem* (McGraw-Hill, New York, 1967); N. H. March, W. H. Young, and S. Sampanthar, *The Many-Body Problem in Quantum Mechanics* (Cambridge University, Cambridge, 1967); G. E. Brown, *Many-Body Problems* (North-Holland, Amsterdam, 1972).

[2]A. A. Abrikosov, L. P. Gorkov, and I. E. Dzyaloshinski, *Methods of Quantum Field Theory in Statistical Physics* (Prentice-Hall, Englewood Cliffs, N.J. 1963).

[3]P. Nozières, *Interacting Fermi Systems* (Benjamin, New York, 1964).

[4]A. B. Migdal, *Theory of Finite Fermi Systems* (Wiley-Interscience, New York, 1967).

[5]D. A. Pines, *The Many-Body Problem* (Benjamin, London, 1962).

[6]A. L. Fetter and J. D. Walecka, *Quantum Theory of Many-Particle Systems* (McGraw-Hill, New York, 1971).

[7]P. C. Martin and J. Schwinger, Phys. Rev. $\underline{115}$, 1342 (1959).

[8]E. E. Salpeter and H. A. Bethe, Phys. Rev. $\underline{84}$, 1232 (1951).

[9]D. J. Rowe, Rev. Mod. Phys. $\underline{40}$, 153 (1968).

[10]C. W. McCurdy, T. N. Rescigno, D. L. Yeager, and V. McKoy, in *Methods of Electronic Structure Theory*, edited by H. F. Schaefer (Plenum, New York, 1977).

[11]D. Goscinski and B. Lukman, Chem. Phys. Lett. $\underline{7}$, 573 (1970); P. Jørgensen, Annu. Rev. Phys. Chem. $\underline{26}$, 359 (1975).

[12]J. Oddershede, Adv. Quantum Chem. $\underline{11}$, 275 (1978).

[13]G. E. Brown, *Unified Theory of Nuclear Models and Forces* (North-Holland, Amsterdam, 1967).

[14]D. J. Thouless, Nucl. Phys. $\underline{22}$, 78 (1961).

[15]V. Gillet, in *Many-Body Description of Nuclear Structure and Reactions,* edited by C. Bloch (Academic, New York, 1967), p. 82; A. M. Green, Rep. Prog. Phys. $\underline{28}$, 113 (1965).

[16]P. L. Altick and A. E. Glassgold, Phys. Rev. 133, A632 (1964).

[17]T. H. Dunning and V. McKoy, J. Chem. Phys. $\underline{47}$, 1735 (1967); *ibid.* $\underline{48}$, 5263 (1968).

[18]P. Ring and P. Schuck, *The Nuclear Many-Body Problem* (Springer, Heidelberg, 1980).

[19]J. Rose, T. Shibuya, and V. McKoy, J. Chem. Phys. $\underline{58}$, 74 (1973).

[20]J. Sawicki, Phys. Rev. $\underline{126}$, 2231 (1962).

[21]T. Tamura and T. Udagawa, Nucl. Phys. $\underline{53}$, 33 (1964).

[22]B. R. Barett, Nucl. Phys. $\underline{A109}$, 129 (1968).

[23]T. Shibuya and V. McKoy, Phys. Rev. $\underline{A2}$, 2208 (1970); T. Shibuya, J. Rose, and V. McKoy, J. Chem. Phys. $\underline{58}$, 500 (1973).

[24]B. Schneider, H. S. Taylor, and R. Yaris, Phys. Rev. $\underline{A1}$, 855 (1970); J. O. Zwicker and R. Yaris, J. Chem. Phys. $\underline{62}$, 1276 (1975).

[25]P. Schuck and S. Ethofer, Nucl. Phys. A $\underline{212}$, 269 (1973).

[26]J. Paldus and J. Čisek, J. Chem. Phys. $\underline{60}$, 149 (1974).

[27]A. C. Lasaga and M. Karplus, Phys. Rev. A $\underline{16}$, 807 (1977).

[28]J. Oddershede and P. Jørgensen, J. Chem. Phys. $\underline{66}$, 1541 (1977).

[29]G. Wegman, Z. Phys. $\underline{226}$, 60 (1969).

[30]W. Brenig, in *Advances in Theoretical Physics,* edited by K. A. Brueckner (Academic, New York, 1965), Vol. 1.